

Coexistence of spin-triplet superconductivity with magnetism within a single mechanism for orbitally degenerate correlated electrons: statistically consistent Gutzwiller approximation

M Zegrodnik¹, J Spalek^{1,2} and J Bünnemann³

¹ AGH University of Science and Technology, Faculty of Physics and Applied Computer Science, Al. Mickiewicza 30, PL-30-059 Kraków, Poland

² Marian Smoluchowski Institute of Physics, Jagiellonian University, Ulica Reymonta 4, PL-30-059 Kraków, Poland

³ Max-Planck Institute for Solid State Research, Heisenbergstrasse 1, D-70569 Stuttgart, Germany

E-mail: michal.zegrodnik@gmail.com, ufspalek@if.uj.edu.pl and buenemann@gmail.com

New Journal of Physics **15** (2013) 073050 (22pp)

Received 1 March 2013

Published 26 July 2013

Online at <http://www.njp.org/>

doi:10.1088/1367-2630/15/7/073050

Abstract. An orbitally degenerate two-band Hubbard model is analyzed with the inclusion of the Hund's rule-induced spin-triplet even-parity paired states and their coexistence with magnetic ordering. The so-called *statistically consistent Gutzwiller approximation* (SGA) has been applied to the case of a square lattice. The superconducting gaps, the magnetic moment and the free energy are analyzed as a function of the Hund's rule coupling strength and the band filling. Also, the influence of the intersite hybridization on the stability of paired phases is discussed. In order to examine the effect of correlations the results are compared with those calculated earlier within the Hartree–Fock (HF) approximation combined with the Bardeen–Cooper–Schrieffer (BCS) approach. Significant differences between the two methods used (HF+BCS versus SGA+real-space pairing) appear in the stability regions of the considered phases. Our results supplement the analysis of this canonical model used



Content from this work may be used under the terms of the [Creative Commons Attribution 3.0 licence](https://creativecommons.org/licenses/by/3.0/). Any further distribution of this work must maintain attribution to the author(s) and the title of the work, journal citation and DOI.

widely in the discussions of pure magnetic phases with the detailed elaboration of the stability of the spin-triplet superconducting states and the coexistent magnetic-superconducting states. At the end, we briefly discuss qualitatively the factors that need to be included for a detailed quantitative comparison with the corresponding experimental results.

Contents

1. Introduction	2
2. Model and method	4
2.1. Statistically consistent Gutzwiller method for superconducting and coexistent superconducting-ferromagnetic phases	8
2.2. Statistically consistent Gutzwiller method for the coexistent antiferromagnetic-spin-triplet superconducting phase	11
3. Results and discussion	14
4. Conclusions	20
Acknowledgments	21
References	21

1. Introduction

The question of coexistence of magnetism and superconductivity appears very often in correlated electron systems. In this context, both the spin-singlet and the spin-triplet paired states should be considered. A general motivation for considering the spin-triplet pairing is provided by the discoveries of superconductivity in Sr_2RuO_4 [1, 2], UGe_2 [3, 4], URhGe [5], UIr [6] and UCoGe [7–9]. In the last four compounds, superconductivity indeed coexists with ferromagnetism. Additionally, for the spin-singlet high-temperature superconductors and heavy-fermion systems, the antiferromagnetism and the superconductivity can have the same origin. Hence, it is natural to ask whether ferromagnetism and the spin-triplet superconductivity also have the same origin in the itinerant uranium ferromagnets. A related and a very non-trivial question concerns the coexistence of antiferromagnetism with the triplet superconducting state as in UNi_2Al_3 [10–12] and UPt_3 [13, 14].

It has previously been argued [15–19]⁴ that for the case of indistinguishable fermions, the intra-atomic Hund’s rule exchange can lead in a natural manner to the coexistence of spin-triplet superconductivity with magnetic ordering—ferromagnetism or antiferromagnetism in the simplest situations. This idea was subsequently elaborated by Zegrodnik and Spalek [20–22] by means of the combined Hartree–Fock (HF)–Bardeen–Cooper–Shrieffer (BCS) approach. In particular, phase diagrams have been determined which contain regions of stability of the pure superconducting phase of type A (i.e. the equal-spin-paired phase), as well as superconductivity coexisting with either ferromagnetism or antiferromagnetism.

The HF approximation, as a rule, overestimates the stability of phases with a broken symmetry. Therefore, in this work, we apply the Gutzwiller approximation (GA) for the same selection of phases in order to go beyond the HF–BCS analysis and examine explicitly the

⁴ For previous brief and qualitative considerations of the ferromagnetism and spin-triplet pairing coexistence see [19].

effects of interelectronic correlations. The extension of the Gutzwiller method to the multi-band case [23–25] provides us with the so-called renormalization factors for our degenerate two-band model. With these factors, we construct an effective Hamiltonian by means of the *statistically consistent Gutzwiller approximation* (SGA) in which additional constraints are added to the standard GA and with the incorporation of which the single-particle state has been determined (see [26–29] for exemplary applications of the SGA method). The detailed phase diagram and the corresponding order parameters are calculated as functions of the microscopic parameters such as the band filling, n , the Hund's rule exchange integral, J , and the intra- and inter-orbital Hubbard interaction parameters, U and U' , respectively. The obtained results are compared with those coming out from the HF approximation. In this manner, the paper extends the discussion of itinerant magnetism within the canonical (extended Hubbard) model, appropriate for this purpose, to the analysis of pure and coexisting superconducting-magnetic states within a single unified approach. It should be noted that theoretical investigations regarding the spin-triplet pairing have been performed recently also for other systems [30–35].

The present model is based on assuming that the starting (bare) bands originate from equivalent orbitals and become inequivalent when the interband hybridization is included. The real 3d or 4d orbitals are anisotropic, so the model requires some extensions to become applicable in a quantitative manner for real materials. We can say that here we discuss thus some universal stability conditions of the paired and coexistent magnetic-paired states, as well as provide some basic quantitative characteristics. This is because, as we show explicitly below, the order parameters and related other quantities are determined by a minimization of either the ground state or free-energy functional which is obtained by integrating $\ln Z$, where Z is the effective grand-canonical partition function, over the single particle effective band energies. Hence, the global energies are averaged out over the band states. In other words, the present model with symmetric bands can be regarded as reflecting qualitative features of Sr_2RuO_4 within a two-band approximation. Nevertheless, it is directly applicable for discussing the superfluidity and magnetism in the two-orbital $SU(4)$ model of multicomponent ultracold fermions [36–38] as the orbitals are identical and the general orbital and the spin symmetry combine to $SU(N)$ symmetry.

The extension of the present model to the uranium system such as UGe_2 would require considering orbitally degenerate and correlated $5f^2$ – $5f^3$ quasi-atomic states due to U and hybridized with the uncorrelated conduction band states. This means that we must have minimally a three-orbital system with two partially occupied 5f quasi-atomic states (so the Hund's rule becomes operative) and at least one extra conduction band. Such a situation may lead to a partial Mott-localization phenomenon, i.e. to a spontaneous decomposition of $5f^n$ ($n > 1$) configuration of electrons into the localized and the itinerant parts [39]. In such a situation, it is possible that the localized electrons are the source of ferromagnetism, whereas the itinerant particles are paired [9]. The last variant of the multiple-band model would be also very useful in the discussion of heavy-fermion compounds. Moreover, in the systems represented by this model, the coexistence of antiferromagnetism and superconductivity has been shown to appear in both experiment [40] and theory [41]. As said above, here we study in detail only the two-orbital situation.

In relation to the even-parity spin-triplet real-space pairing, discussed here and induced by the Hund's rule, one should also mention the spin fluctuations as another possible mechanism of spin-triplet pairing, which appears in liquid ^3He [42] and other systems. In that case, if the spin-triplet pairing is taking place in a single band, the paired states must be then of odd parity.

Within the present approach the spin fluctuations should be treated as quantum fluctuations around the present self-consistently renormalized mean-field state [43], and hence are regarded as processes of higher order.

The paper is composed as follows. In section 2, we provide the principal aspects of real-space spin-triplet pairing induced by the Hund's rule coupling, and introduce the band-renormalization factors for our two-band model. Furthermore, in sections 2.1 and 2.2 of section 2 we explain how the effective Hamiltonian is constructed, according to the SGA, for all the phases considered in this work. In section 3 we discuss the phase diagram, and the principal order parameters in the considered phases, whereas section 4 contains the concluding remarks.

2. Model and method

We consider the extended orbitally degenerate Hubbard Hamiltonian, which has the form

$$\begin{aligned}\hat{H} &= \sum_{ij(i \neq j)ll'\sigma} t_{ij}^{ll'} \hat{c}_{il\sigma}^\dagger \hat{c}_{jl'\sigma} + (U' + J) \sum_i \hat{n}_{i1} \hat{n}_{i2} \\ &\quad + U \sum_{il} \hat{n}_{il\uparrow} \hat{n}_{il\downarrow} - J \sum_{ill'(l \neq l')} \left(\hat{\mathbf{S}}_{il} \cdot p \hat{\mathbf{S}}_{il'} + \frac{3}{4} \hat{n}_{il} \hat{n}_{il'} \right) \\ &= \hat{H}^0 + \hat{H}^{\text{at}},\end{aligned}\quad (1)$$

where $l = 1, 2$ label the orbitals and the first term describes electron hopping between atomic sites i and j . For $l \neq l'$ this term represents electron hopping with change of the orbital (i.e. hybridization in momentum space). The next two terms describe the Coulomb interactions between electrons on the same atomic site. However, the second term also contains the contribution, originating from the exchange interaction (J). The last term expresses the Hund's rule, i.e. the ferromagnetic exchange between electrons localized on the same site, but on different orbitals. This term contributes to magnetic coupling and is responsible for the spin-triplet pairing leading to magnetic ordering, superconductivity and coexistent magnetic-superconducting phases. In the Hamiltonian (1), we have disregarded the pair hopping term $(J/2) \sum_{il \neq l'} \hat{c}_{il\uparrow}^\dagger \hat{c}_{il\downarrow}^\dagger \hat{c}_{il'\downarrow} \hat{c}_{il'\uparrow}$ and the so-called correlated hopping term $\sim V \sum_{il \neq l'} \hat{n}_{il\bar{\sigma}} (\hat{c}_{il\sigma}^\dagger \hat{c}_{il'\sigma} + \text{h.c.})$. This is because their magnitude depends on the double occupancy probability which is small for $U > W$ (see below), where W is the bare bandwidth. Additionally the coupling constant V for e_g , 3d orbitals is smaller than $J \approx 4V$ [44].

In our variational method, we assume that the correlated state $|\Psi_G\rangle$ of the system can be expressed in the following manner:

$$|\Psi_G\rangle = \hat{P}_G |\Psi_0\rangle, \quad (2)$$

where $|\Psi_0\rangle$ is the normalized non-correlated state to be determined later and \hat{P}_G is the Gutzwiller correlator selected in the following form:

$$\hat{P}_G = \prod_i \hat{P}_{G|i} = \prod_i \sum_{I, I'} \lambda_{I, I'}^{(i)} |I\rangle_{ii} \langle I'|. \quad (3)$$

Here, $\lambda_{I, I'}^{(i)}$ are the variational parameters, which are assumed to be real. In the two-band situation the local basis consists of 16 states (see table 1), which are defined as follows:

$$|I\rangle_i = \hat{C}_{i, I}^\dagger |0\rangle_i \equiv \prod_{\gamma \in I} \hat{c}_{i\gamma}^\dagger |0\rangle_i = \hat{c}_{i\gamma_1}^\dagger \dots \hat{c}_{i\gamma_{|I|}}^\dagger |0\rangle_i, \quad (4)$$

Table 1. The local basis consisting of 16 configurations containing $N_e = 0, \dots, 4$ electrons, which are enumerated as shown below.

$ 0, 0\rangle$	1	$ 0, \downarrow\rangle$	5	$ \downarrow, \downarrow\rangle$	9	$ \uparrow\downarrow, \uparrow\rangle$	13
$ \uparrow, 0\rangle$	2	$ \uparrow\downarrow, 0\rangle$	6	$ \uparrow, \downarrow\rangle$	10	$ \downarrow, \uparrow\downarrow\rangle$	14
$ 0, \uparrow\rangle$	3	$ 0, \uparrow\downarrow\rangle$	7	$ \downarrow, \uparrow\rangle$	11	$ \uparrow\downarrow, \downarrow\rangle$	15
$ \downarrow, 0\rangle$	4	$ \uparrow, \uparrow\rangle$	8	$ \uparrow, \uparrow\downarrow\rangle$	12	$ \uparrow\downarrow, \uparrow\downarrow\rangle$	16

where $\gamma = 1, 2, 3, 4$ labels the four spin-orbital states (in the $l\sigma$ notation: $1\uparrow, 1\downarrow, 2\uparrow, 2\downarrow$, respectively) and $|I|$ is the number of electrons in the local state $|I\rangle$. In general, an index I can be interpreted as a set in the usual mathematical sense. The creation operators in (4) are placed in ascending order, i.e. $\gamma_1 < \dots < \gamma_{|I|}$. In an analogous manner, one can define the product of annihilation operators

$$\hat{C}_{i,I} = \prod_{\gamma \in I} \hat{c}_{i\gamma} = \hat{c}_{i\gamma_1} \dots \hat{c}_{i\gamma_{|I|}} \quad (5)$$

which are placed in the descending order $\gamma_1 > \dots > \gamma_{|I|}$.

The operator $|I\rangle_{ii}\langle I'|$ can be expressed in terms of \hat{C}_I^\dagger and \hat{C}_I in the following manner:

$$\hat{m}_{I,I'|i} \equiv |I\rangle_{ii}\langle I'| = \hat{C}_{i,I}^\dagger \hat{C}_{i,I'} \hat{n}_{I \cup I'|i}^h, \quad (6)$$

where

$$\hat{n}_{I \cup I'|i}^h = \prod_{\gamma \in \overline{I \cup I'}} (1 - \hat{n}_{i\gamma}). \quad (7)$$

In the subsequent discussion, we write expectation values with respect to $|\Psi_0\rangle$ as

$$\langle \hat{O} \rangle_0 = \langle \Psi_0 | \hat{O} | \Psi_0 \rangle \quad (8)$$

while the expectation values with respect to $|\Psi_G\rangle$ will be denoted by

$$\langle \hat{O} \rangle_G = \frac{\langle \Psi_G | \hat{O} | \Psi_G \rangle}{\langle \Psi_G | \Psi_G \rangle}. \quad (9)$$

The most important step within the Gutzwiller approach is to derive the formula for the expectation value of the Hamiltonian $\hat{K} = \hat{H} - \mu \hat{N}$ with respect to $|\Psi_G\rangle$. This can be done in the limit of infinite dimensions by a diagrammatic approach [25] which uses the variational analogue of Feynmann diagrams. By applying this method to the interaction part of the Hamiltonian (1), which is completely of intra-site character, one obtains

$$\langle \hat{H}^{\text{at}} \rangle_G = L \sum_{I_1, I_4} \bar{E}_{I_1, I_4} \langle \hat{m}_{I_1, I_4} \rangle_0, \quad (10)$$

where

$$\bar{E}_{I_1, I_4} = \sum_{I_2, I_3} \lambda_{I_1, I_2} \lambda_{I_3, I_4} \langle I_2 | \hat{H}^{\text{at}} | I_3 \rangle \quad (11)$$

and L is the number of atomic sites. In (10) we have assumed that our system is homogeneous. Note that with the use of Wick's theorem, the purely local expectation values $\langle \hat{m}_{I_1, I_4} \rangle_0$ can be

expressed in terms of the local single-particle density matrix elements $\langle \hat{c}_{i\gamma}^\alpha \hat{c}_{i\gamma'}^{\alpha'} \rangle_0$. Here, $\hat{c}_{i\gamma}^\alpha$ are either creation or annihilation operators.

The expectation value of the single-particle part in the Hamiltonian (1) can be cast to the form

$$\langle \hat{H}^0 \rangle_G = \sum_{ij (i \neq j)} \sum_{\gamma \gamma' \tilde{\gamma} \tilde{\gamma}'} t_{ij}^{\gamma \gamma'} (q_{\gamma \tilde{\gamma}} q_{\gamma' \tilde{\gamma}'} - \bar{q}_{\gamma \tilde{\gamma}} \bar{q}_{\gamma' \tilde{\gamma}'}) \langle \hat{c}_{i, \tilde{\gamma}}^\dagger \hat{c}_{j, \tilde{\gamma}'} \rangle_0, \quad (12)$$

where we have assumed that the renormalization factors q and \bar{q} are real numbers and $t^{\gamma \gamma'} = t^{\gamma' \gamma}$. Moreover, in the equation above we have neglected the part containing the inter-site pairing terms $\langle \hat{c}_{i, \gamma}^\dagger \hat{c}_{j, \gamma'}^\dagger \rangle_0$ and $\langle \hat{c}_{i, \gamma} \hat{c}_{j, \gamma'} \rangle_0$ as we are going to concentrate on the Hund's rule-induced intra-site spin-triplet paired states. The inter-site pairing amplitudes are much smaller than the intra-site terms, in the considered model. The renormalization factors, introduced in (12), have the form

$$q_{\gamma \tilde{\gamma}} = \sum_{I (\tilde{\gamma} \notin I)} \left[\sum_{I'} \text{fsgn}(\tilde{\gamma}, I) m_{I, I'}^{0(\tilde{\gamma})} c_{I \cup \tilde{\gamma}, I' | \gamma}^* + \sum_{I' (\tilde{\gamma} \notin I')} \text{fsgn}(\tilde{\gamma}, I) m_{I', I \cup \tilde{\gamma}}^0 c_{I', I | \gamma}^* \right], \quad (13)$$

where $m_{I, I'}^0 = \langle \hat{m}_{I, I'} \rangle_0$ and $m_{I, I'}^{0(\tilde{\gamma})} = \langle \hat{m}_{I, I'}^{(\tilde{\gamma})} \rangle_0$. Here we have introduced the operator

$$\hat{m}_{I, I'}^{(\gamma)} = \hat{C}_{i, I}^\dagger \hat{C}_{i, I'} \hat{n}_{I \cup I' \cup \gamma | i}^h. \quad (14)$$

The parameters $c_{I_1, I_2 | \gamma}^*$ in (13) are defined as

$$c_{I_1, I_2 | \gamma}^* = \sum_{I (\gamma \notin I)} \text{fsgn}(\gamma, I) \lambda_{I_1, I \cup \gamma} \lambda_{I, I_2}, \quad (15)$$

where we introduced the fermionic sign function

$$\text{fsgn}(\gamma, I) \equiv \langle I \cup \gamma | \hat{c}_\gamma^\dagger | I \rangle. \quad (16)$$

The renormalization factors $\bar{q}_{\gamma \tilde{\gamma}}$ have to be included in (12), when there are non-zero gap parameters ($\langle \hat{c}^\alpha \hat{c}^\alpha \rangle_0 \neq 0$) in $|\Psi_0\rangle$, which is the case considered here. The form of $\bar{q}_{\gamma \tilde{\gamma}}$ is as follows:

$$\bar{q}_{\gamma \tilde{\gamma}} = \sum_{I (\tilde{\gamma} \notin I)} \left[\sum_{I'} \text{fsgn}(\tilde{\gamma}, I) m_{I', I}^{0(\tilde{\gamma})} c_{I', I \cup \tilde{\gamma} | \gamma}^* + \sum_{I' (\tilde{\gamma} \notin I')} \text{fsgn}(\tilde{\gamma}, I) m_{I \cup \tilde{\gamma}, I'}^0 c_{I', I | \gamma}^* \right]. \quad (17)$$

The remaining part of $\langle \hat{K} \rangle_G$ that has to be derived is the expectation value $\langle \hat{N} \rangle_G$. Also in this case, the diagrammatic evaluation in infinite dimensions gives the proper formula

$$\langle \hat{N} \rangle_G = \sum_{i\gamma} \langle \hat{n}_{i\gamma} \rangle_G, \quad (18)$$

where

$$\langle \hat{n}_{i\gamma} \rangle_G = \sum_{I_1, I_4} N_{I_1, I_4}^\gamma m_{I_1, I_4}^0 \quad (19)$$

and

$$N_{I_1, I_4}^\gamma = \sum_{I (\gamma \notin I)} \lambda_{I_1, I \cup \gamma} \lambda_{I \cup \gamma, I_4}. \quad (20)$$

The pairing densities in the correlated state that are going to be useful in the subsequent discussion can be expressed in the following way:

$$\langle \hat{c}_{i\gamma} \hat{c}_{i\gamma'} \rangle_G = \sum_{I_1, I_4} S_{I_1, I_4}^{\gamma\gamma'} m_{I_1, I_4}^0, \quad (21)$$

where

$$S_{I_1, I_4}^{\gamma\gamma'} = \sum_{I(\gamma\gamma' \notin I)} \lambda_{I_1, I} \lambda_{I \cup (\gamma\gamma'), I_4} \text{fsgn}(\gamma, I) \text{fsgn}(\gamma', I) \text{fsgn}(\gamma', \gamma). \quad (22)$$

Using (10), (12) and (18) one can express $\langle \hat{K} \rangle_G$ in terms of the variational parameters $\lambda_{I, I'}$, local and non-local single-particle density matrix elements, $\langle \hat{c}_{i\gamma}^\alpha \hat{c}_{i\gamma'}^{\alpha'} \rangle_0$, $\langle \hat{c}_{i,\gamma}^\dagger \hat{c}_{j,\gamma'} \rangle_0$ and the matrix elements of the atomic part of the atomic Hamiltonian represented in the local basis $\langle I | \hat{H}^{\text{at}} | I' \rangle$.

The formula for $\langle \hat{K} \rangle_G$, obtained in the way described above, can be written as an expectation value of an effective Hamiltonian \hat{K}_{GA} , evaluated with respect to $|\Psi_0\rangle$

$$\begin{aligned} \hat{K}_{\text{GA}} = & \sum_{ij(i \neq j)} \sum_{\gamma\gamma'\tilde{\gamma}\tilde{\gamma}'} t_{ij}^{\gamma\gamma'} (q_{\gamma\tilde{\gamma}} q_{\gamma'\tilde{\gamma}'} - \bar{q}_{\gamma\tilde{\gamma}} \bar{q}_{\gamma'\tilde{\gamma}'}) \hat{c}_{i,\tilde{\gamma}}^\dagger \hat{c}_{j,\tilde{\gamma}'} \\ & - \mu \sum_{i\gamma} q_\gamma^s \hat{n}_{i\gamma} + L \sum_{I_1, I_4} \bar{E}_{I_1, I_4} \langle \hat{m}_{I_1, I_4} \rangle_0, \end{aligned} \quad (23)$$

where $q_\gamma^s = \langle \hat{n}_{i\gamma} \rangle_G / \langle \hat{n}_{i\gamma} \rangle_0$. There is no guarantee that the condition

$$\langle \hat{n}_{i\gamma} \rangle_G = \langle \hat{n}_{i\gamma} \rangle_0 \quad (24)$$

is fulfilled. It turns out that it is fulfilled for the paramagnetic and the magnetically ordered phases of our two-band system; however, it is not for the superconducting phases. Physically, it is most sensible to fix $\langle \hat{n} \rangle_G$ instead of $\langle \hat{n} \rangle_0$, during the minimization. This is the reason why we include the term $-\mu \hat{N}$ already at the beginning of our derivation in $\langle \hat{K} \rangle_G$. In this manner the chemical potential μ refers to the initial correlated system, not to the effective non-correlated one (for which the chemical potential can be different).

Having in mind that there are 16 states in the local basis there could be up to $16 \times 16 = 256$ variational parameters $\lambda_{I, I'}$. However, for symmetry reasons many of these parameters are zero. The finite parameters can be identified by the following rule:

$$\lambda_{I, I'} \neq 0 \Leftrightarrow \langle \hat{m}_{I, I'} \rangle_0 \neq 0 \vee \langle I | \hat{H}^{\text{at}} | I' \rangle \neq 0. \quad (25)$$

It should also be noted that, as shown in [25], the variational parameters are not independent since they have to obey the constraints:

$$\begin{aligned} \langle \hat{P}_{G|i}^2 \rangle_0 &= 1, \\ \langle \hat{c}_{i\gamma}^\dagger \hat{P}_{G|i}^2 \hat{c}_{i\gamma'} \rangle_0 &= \langle \hat{c}_{i\gamma}^\dagger \hat{c}_{i\gamma'} \rangle_0, \\ \langle \hat{c}_{i\gamma}^\dagger \hat{P}_{G|i}^2 \hat{c}_{i\gamma'}^\dagger \rangle_0 &= \langle \hat{c}_{i\gamma}^\dagger \hat{c}_{i\gamma'}^\dagger \rangle_0, \\ \langle \hat{c}_{i\gamma} \hat{P}_{G|i}^2 \hat{c}_{i\gamma'} \rangle_0 &= \langle \hat{c}_{i\gamma} \hat{c}_{i\gamma'} \rangle_0 \end{aligned} \quad (26)$$

which are going to be used to fix some of the parameters $\lambda_{I, I'}$.

The results presented in this work have been obtained for the case of a square lattice with the band dispersions

$$\epsilon_{1\mathbf{k}} = \epsilon_{2\mathbf{k}} \equiv \epsilon_{\mathbf{k}} = 2t(\cos(k_x) + \cos(k_y)) \quad (27)$$

and also

$$\epsilon_{12\mathbf{k}} = \epsilon_{21\mathbf{k}} = \beta_h \epsilon_{\mathbf{k}}, \quad (28)$$

where $\beta_h \in [0, 1]$. The orbital degeneracy and spatial homogeneity allow us to write

$$\begin{aligned} \langle \hat{n}_{i1} \rangle_G &= \langle \hat{n}_{i2} \rangle_G \equiv n_G/2, \\ \langle \hat{S}_{i1}^z \rangle_G &= \langle \hat{S}_{i2}^z \rangle_G \equiv S_G^z, \end{aligned} \quad (29)$$

where

$$\begin{aligned} \hat{S}_{il}^z &\equiv \frac{1}{2}(\hat{n}_{il\uparrow} - \hat{n}_{il\downarrow}), \\ \hat{n}_{il} &\equiv \hat{n}_{il\uparrow} + \hat{n}_{il\downarrow}. \end{aligned} \quad (30)$$

Similar expressions as in (29) can be introduced for the expectation values in the non-correlated state $|\Psi_0\rangle$.

Before discussing the principal magnetic and/or spin-triplet superconducting phases, we introduce first the exact expression of the full exchange operator (the last term of our Hamiltonian) via the local spin-triplet pairing operators ($\hat{A}_{im}^\dagger, \hat{A}_{im}$) namely

$$\sum_{ll' (l \neq l')} (\hat{\mathbf{S}}_{il} \cdot \hat{\mathbf{S}}_{il'} + \frac{3}{4} \hat{n}_{il} \hat{n}_{il'}) = \sum_m \hat{A}_{im}^\dagger \hat{A}_{im}, \quad (31)$$

where

$$\hat{A}_{i,m}^\dagger \equiv \begin{cases} a_{i1\uparrow}^\dagger a_{i2\uparrow}^\dagger, & m = 1, \\ a_{i1\downarrow}^\dagger a_{i2\downarrow}^\dagger, & m = -1, \\ \frac{1}{\sqrt{2}}(a_{i1\uparrow}^\dagger a_{i2\downarrow}^\dagger + a_{i1\downarrow}^\dagger a_{i2\uparrow}^\dagger), & m = 0. \end{cases} \quad (32)$$

We see that those two representations are mathematically equivalent, so the phase with $S_G^z = \langle \hat{S}_{il}^z \rangle_G \neq 0$ and that with the corresponding off-diagonal order parameter $\langle \hat{A}_{im} \rangle_G \neq 0$ (or $\langle \hat{A}_{im}^\dagger \rangle_G \neq 0$) should be treated on equal footing.

2.1. Statistically consistent Gutzwiller method for superconducting and coexistent superconducting-ferromagnetic phases

In this subsection we will describe the SGA approach as applied to the selected phases characterized by the following order parameters:

- Superconducting phase of type A1 coexisting with ferromagnetism (A1 + FM).
 $S_{G|u}^z \neq 0, \Delta_1^G \neq 0, \Delta_{-1}^G = \Delta_0^G = 0.$
- Pure type A superconducting phase (A).
 $S_{G|u}^z = 0, \Delta_1^G = \Delta_{-1}^G \neq 0, \Delta_0^G = 0.$
- Pure ferromagnetic phase (FM).
 $S_{G|u}^z \neq 0, \Delta_1^G = \Delta_{-1}^G = \Delta_0^G = 0,$
- Paramagnetic phase (NS).
 $S_{G|u}^z = 0, \Delta_1^G = \Delta_{-1}^G = \Delta_0^G = 0,$

Table 2. Non-zero, off-diagonal local variational parameters ($\lambda_{I,I'} = \lambda_{I',I}$) that are used in the calculations for the considered phases.

I	1	2	3	4	5	8	9	8	10	1	1
I'	16	15	14	13	12	16	16	9	11	8	9

where $S_{G|u}^z$ refers to the uniform magnetic moment and

$$\Delta_m^G = \langle \hat{A}_{im} \rangle_G, \quad (\Delta_m^G)^* = \langle \hat{A}_{im}^\dagger \rangle_G \quad (33)$$

are the spin-triplet local gap parameters that are assumed as real here.

The (correlated) order parameters that have been used above to define the relevant phases can also be defined for the non-correlated state $|\Psi_0\rangle$. With these, we can determine which of the matrix elements $\langle \hat{m}_{I,I'} \rangle_0$ are equal to zero for the considered phases. Assumption (25) then allows us to choose the non-diagonal variational parameters, $\lambda_{I,I'}$, that have to be taken into account during the calculations. We list their indices (I, I') in table 2.

As one can see from table 2, the off-diagonal variational parameters correspond to the creation or annihilation of the Cooper pair in the proper spin-triplet states $|1 \uparrow, 2 \uparrow\rangle$ and $|1 \downarrow, 2 \downarrow\rangle$ (phase A). Because in the A1 phase only electrons with spin up are paired, one can assume that $\lambda_{1,16}, \lambda_{2,15}, \lambda_{3,14}, \lambda_{8,16}, \lambda_{8,9}$ are zero (and their transposed correspondents— $\lambda_{I,I'} = \lambda_{I',I}$). For the FM and NS, unpaired states only $\lambda_{10,11}$ and $\lambda_{11,10}$ are non-zero. They correspond to the two non-diagonal matrix elements of the atomic Hamiltonian, $\langle I | \hat{H}^{\text{at}} | I' \rangle$. With the information contained in table 2, one obtains the following relations regarding the band-narrowing renormalization factors:

$$\begin{aligned} q_{l\sigma, l'\sigma'} &\neq 0 \Leftrightarrow l = l' \wedge \sigma = \sigma', \\ \bar{q}_{l\sigma, l'\sigma'} &\neq 0 \Leftrightarrow l \neq l' \wedge \sigma = \sigma', \end{aligned} \quad (34)$$

where we have again used the $\gamma = l\sigma$ notation. Owing to the degeneracy of our bands we find that

$$\begin{aligned} q_{1\sigma, 1\sigma} &= q_{2\sigma, 2\sigma} \equiv q_\sigma, \\ \bar{q}_{1\sigma, 2\sigma} &= -\bar{q}_{2\sigma, 1\sigma} \equiv \bar{q}_\sigma, \\ q_{1\sigma}^s &= q_{2\sigma}^s \equiv q_\sigma^s. \end{aligned} \quad (35)$$

Using the equations above we can rewrite the Hamiltonian (23) in the more explicit form, in reciprocal space

$$\hat{K}_{\text{GA}} = \sum_{\mathbf{k}l\sigma} (Q_\sigma \epsilon_{\mathbf{k}} - q_\sigma^s \mu) \hat{n}_{\mathbf{k}l\sigma} + \sum_{\mathbf{k}l'l'(\neq l')\sigma} Q_\sigma \epsilon_{\mathbf{k}12} \hat{c}_{\mathbf{k}l\sigma}^\dagger \hat{c}_{\mathbf{k}l'\sigma} + L \sum_{I_1, I_4} \bar{E}_{I_1, I_4} \langle \hat{m}_{I_1, I_4} \rangle_0, \quad (36)$$

where the renormalization factors Q_σ are defined as

$$Q_\sigma \equiv q_\sigma^2 - \bar{q}_\sigma^2. \quad (37)$$

Having the formula for \hat{K}_{GA} , given by (36), one can introduce next the so-called SGA. In this method, the mean fields (such as the expectation values for magnetization or superconducting gaps) are treated as variational mean-field order parameters with respect to which the energy of the system is minimized. However, in order to make sure that they coincide with the corresponding values calculated self-consistently, additional constraints have

to be introduced with the help of the Lagrange-multiplier method [26–29]. This leads to the supplementary terms in the effective Hamiltonian of the following form:

$$\begin{aligned}\hat{K}_\lambda = & \hat{K}_{\text{GA}} - \sum_{m=\pm 1} \left[\lambda_m \left(\sum_{\mathbf{k}} \hat{A}_{\mathbf{k}m} - L \Delta_m^0 \right) + \text{h.c.} \right] \\ & - \lambda_S \left(\sum_{\mathbf{k}l} \hat{S}_{\mathbf{k}l}^z - 2L S_0^z \right) - \lambda_n \left(\sum_{\mathbf{k}l\sigma} q_{l\sigma}^s \hat{n}_{\mathbf{k}l\sigma} - L n_G \right),\end{aligned}\quad (38)$$

where the Lagrange multipliers λ_m , λ_S and λ_n are introduced to assure, respectively, that the averages $\langle \hat{A}_{\mathbf{k}m} \rangle$, $\langle \hat{S}_{\mathbf{k}l} \rangle$ and $\langle \hat{n}_{\mathbf{k}l\sigma} \rangle$ calculated either from the corresponding self-consistent equations or variationally, coincide with each other, which guarantees the fulfillment of the fundamental Bogoliubov principle (otherwise violated in some cases [29]). In this manner, we do not alter any of the infinite-dimension features of the approach, used to derive the effective ground-state (or the free energy) functional, instead form the consistent (renormalized) mean-field theory of the correlated fermion system at hand.

Introducing the four-component representation of single-particle operators

$$\hat{\mathbf{f}}_{\mathbf{k}\sigma}^\dagger = (\hat{c}_{\mathbf{k}1\sigma}^\dagger, \hat{c}_{\mathbf{k}2\sigma}^\dagger, \hat{c}_{-\mathbf{k}1\sigma}, \hat{c}_{-\mathbf{k}2\sigma}), \quad (39)$$

we can write down the effective Hamiltonian in the following form:

$$\begin{aligned}\hat{K}_\lambda = & \frac{1}{2} \sum_{\mathbf{k}\sigma} \hat{\mathbf{f}}_{\mathbf{k}\sigma}^\dagger \hat{\mathbf{M}}_{\mathbf{k}\sigma} \hat{\mathbf{f}}_{\mathbf{k}\sigma} + \sum_{\mathbf{k}\sigma} \tilde{\epsilon}_{\mathbf{k}\sigma} + 2L \sum_{m=\pm 1} \lambda_m \Delta_m^0 + 2L \lambda_S S_0^z + L \lambda_n n_G \\ & + L \sum_{I_1, I_4} \bar{E}_{I_1, I_4} \langle \hat{m}_{I_1, I_4} \rangle_0,\end{aligned}\quad (40)$$

where $\hat{\mathbf{M}}_{\mathbf{k}\sigma}$ is a 4×4 orthogonal matrix

$$\hat{\mathbf{M}}_{\mathbf{k}\sigma} = \begin{pmatrix} \tilde{\epsilon}_{\mathbf{k}\sigma} & Q_\sigma \epsilon_{\mathbf{k}12} & 0 & \lambda_\sigma \\ Q_\sigma \epsilon_{\mathbf{k}12} & \tilde{\epsilon}_{\mathbf{k}\sigma} & -\lambda_\sigma & 0 \\ 0 & -\lambda_\sigma & -\tilde{\epsilon}_{\mathbf{k}\sigma} & -Q_\sigma \epsilon_{\mathbf{k}12} \\ \lambda_\sigma & 0 & -Q_\sigma \epsilon_{\mathbf{k}12} & -\tilde{\epsilon}_{\mathbf{k}\sigma} \end{pmatrix}. \quad (41)$$

Here we introduced λ_\uparrow and λ_\downarrow which correspond to the Lagrange parameters $\lambda_{m=1}$ and $\lambda_{m=-1}$, respectively. The bare quasi-particle energies $\tilde{\epsilon}_{\mathbf{k}\sigma}$ are defined as

$$\tilde{\epsilon}_{\mathbf{k}\sigma} = Q_\sigma \epsilon_{\mathbf{k}} - q_\sigma^s (\mu + \lambda_n) - \frac{1}{2} \sigma \lambda_S. \quad (42)$$

The diagonalization of the matrix (41) yields the quasiparticle eigenenergies in the paired states of the following form:

$$\begin{aligned}E_{\mathbf{k}1\sigma} &= \sqrt{\tilde{\epsilon}_{\mathbf{k}\sigma}^2 + \lambda_\sigma^2} - Q_\sigma \epsilon_{\mathbf{k}12}, \\ E_{\mathbf{k}2\sigma} &= \sqrt{\tilde{\epsilon}_{\mathbf{k}\sigma}^2 + \lambda_\sigma^2} + Q_\sigma \epsilon_{\mathbf{k}12}, \\ E_{\mathbf{k}3\sigma} &= -\sqrt{\tilde{\epsilon}_{\mathbf{k}\sigma}^2 + \lambda_\sigma^2} - Q_\sigma \epsilon_{\mathbf{k}12}, \\ E_{\mathbf{k}4\sigma} &= -\sqrt{\tilde{\epsilon}_{\mathbf{k}\sigma}^2 + \lambda_\sigma^2} + Q_\sigma \epsilon_{\mathbf{k}12}.\end{aligned}\quad (43)$$

The first two energies correspond to the doubly degenerate spin-split quasi-particle excitations in the A phase, whereas the remaining two are their quasihole correspondents.

Even though the Gutzwiller approach was derived for zero temperature, we may construct the grand-potential function F_λ (per atomic site) that corresponds to the effective Hamiltonian (40), i.e.

$$F_\lambda = -\frac{1}{L\beta} \sum_{\mathbf{k}\sigma} \ln [1 + e^{-\beta E_{\mathbf{k}\sigma}}] + \frac{1}{L} \sum_{\mathbf{k}\sigma} \tilde{\epsilon}_{\mathbf{k}\sigma} + 2 \sum_{m=\pm 1} \lambda_m \Delta_m^0 + 2\lambda_S S_0^z + (\lambda_n + \mu)n_G + \sum_{I_1, I_4} \bar{E}_{I_1, I_4} \langle \hat{m}_{I_1, I_4} \rangle_0. \quad (44)$$

The values of the mean fields, the variational parameters and the Lagrange multipliers are found by minimizing the F_λ functional, i.e. the necessary conditions for minimum are

$$\frac{\partial F_\lambda}{\partial \vec{A}} = 0, \quad \frac{\partial F_\lambda}{\partial \vec{\Lambda}_V} = 0, \quad \frac{\partial F_\lambda}{\partial \vec{\Lambda}_L} = 0, \quad (45)$$

where \vec{A} , $\vec{\Lambda}_V$ and $\vec{\Lambda}_L$ denote collectively the mean fields in the non-correlated state, the variational parameters and the Lagrange multipliers, respectively. Additionally, the chemical potential, μ , enters through the relation

$$\frac{\partial F_\lambda}{\partial n_G} = \mu. \quad (46)$$

After solving the complete set of equations, one still has to calculate the mean fields in the correlated state with the use of their analogues in the non-correlated state and the variational parameters using (19) and (21).

With the SGA method one minimizes the variational ground state energy $\langle \hat{K} \rangle_G$ with respect to the variational parameters $\lambda_{I, I'}$ and the single-particle states $|\Psi_0\rangle$. Note that an alternative way for this minimization has been introduced, e.g. in [45]. Beyond the ground-state properties of \hat{K} one is often also interested in the (effective) single-particle Hamiltonian (40) because its eigenvalues are interpreted as quasi-particle excitation energies [46].

2.2. Statistically consistent Gutzwiller method for the coexistent antiferromagnetic-spin-triplet superconducting phase

To consider antiferromagnetism in the simplest case, we divide our system into two interpenetrating sublattices *A* and *B*. In accordance with this division, we define the annihilation operators on the sublattices

$$\hat{c}_{i\sigma} = \begin{cases} \hat{c}_{i\sigma A} & \text{for } i \in A, \\ \hat{c}_{i\sigma B} & \text{for } i \in B. \end{cases} \quad (47)$$

The same holds for the creation operators. Next, the Gutzwiller correlator can be expressed in the form

$$\hat{P}_G = \prod_{i(A)} \hat{P}_{G|i}^{(A)} \prod_{i(B)} \hat{P}_{G|i}^{(B)}, \quad (48)$$

where

$$\hat{P}_{G|i}^{(A/B)} = \sum_{I,I'} \lambda_{I,I'}^{(A/B)} |I\rangle_{ii} \langle I'|. \quad (49)$$

If we assume that charge ordering is absent, we have

$$\langle \hat{S}_{i|A}^z \rangle_G \equiv S_{G|s}^z, \quad \langle \hat{S}_{i|B}^z \rangle_G \equiv -S_{G|s}^z, \quad (50)$$

$$\langle \hat{n}_{i|A} \rangle_G = \langle n_{i|B} \rangle_G \equiv n_G/2. \quad (51)$$

Similar expressions can be obtained for the case of expectation values taken in the state $|\Psi_0\rangle$. As one can see from (49), we have introduced separate sets of variational parameters ($\lambda_{I,I'}^A$ and $\lambda_{I,I'}^B$) for the two sublattices. Fortunately, it does not mean that we have twice as many variational parameters as in the preceding subsection. The parameters $\lambda_{I,I'}^A$ are related to the corresponding $\lambda_{I,I'}^B$ through

$$\lambda_{I_1,I_2}^{(A)} = \lambda_{I_3,I_4}^{(B)}, \quad (52)$$

where the states I_1 and I_2 have opposite spins to those in the I_3 and I_4 states, respectively. The same division has to be made for the renormalization factors q , \bar{q} and q^s . They fulfill the transformation relations

$$\begin{aligned} q_{\gamma,\gamma'}^A &= q_{\bar{\gamma},\bar{\gamma}'}^B, \\ \bar{q}_{\gamma,\gamma'}^A &= \bar{q}_{\bar{\gamma},\bar{\gamma}'}^B, \\ q_{\gamma A}^s &= q_{\bar{\gamma} B}^s, \end{aligned} \quad (53)$$

where γ and $\bar{\gamma}$ are spin-orbitals with opposite spins. The coexistent superconducting-antiferromagnetic phase (SC + AF) can be defined in the following way:

$$\begin{aligned} \Delta_{1A}^G &= \Delta_{-1B}^G \equiv \Delta_+^G \neq 0, \\ \Delta_{-1A}^G &= \Delta_{1B}^G \equiv \Delta_-^G \neq 0, \\ S_{G|s}^z &\neq 0. \end{aligned} \quad (54)$$

Considerations analogical to those presented in section 2 lead to the conclusion that for both sublattices the non-diagonal variational parameters, $\lambda_{I,I'}^A$ and $\lambda_{I,I'}^B$, that have to be used in the calculations, appropriate for the SC + AF phase, are the same as those listed in table 2. This fact, and the degeneracy of our bands, allow us to apply (35) for both sets of renormalization factors (for A and B sublattices), as we have

$$\begin{aligned} q_{1\sigma,1\sigma}^A &= q_{2\sigma,2\sigma}^A = q_{1\bar{\sigma},1\bar{\sigma}}^B = q_{2\bar{\sigma},2\bar{\sigma}}^B \equiv q_\sigma, \\ \bar{q}_{1\sigma,2\sigma}^A &= -\bar{q}_{2\sigma,1\sigma}^A \equiv \bar{q}_\sigma; \quad \bar{q}_{1\bar{\sigma},2\bar{\sigma}}^B = -\bar{q}_{2\bar{\sigma},1\bar{\sigma}}^B \equiv \bar{q}_\sigma, \\ q_{1\sigma A}^s &= q_{2\sigma A}^s = q_{1\bar{\sigma} B}^s = q_{2\bar{\sigma} B}^s \equiv q_\sigma^s, \end{aligned} \quad (55)$$

where $\bar{\sigma}$ represents the spin opposite to σ . Now, we can write down the Hamiltonian \hat{K}_{GA} for the case of SC + AF phase

$$\begin{aligned} \hat{K}_{GA} &= \sum_{\mathbf{k}l\sigma} Q\epsilon_{\mathbf{k}} (\hat{c}_{\mathbf{k}l\sigma A}^\dagger \hat{c}_{\mathbf{k}l\sigma B} + \hat{c}_{\mathbf{k}l\sigma B}^\dagger \hat{c}_{\mathbf{k}l\sigma A}) + \sum_{\mathbf{k}l'l''\sigma} Q\epsilon_{\mathbf{k}12} (\hat{c}_{\mathbf{k}l\sigma A}^\dagger \hat{c}_{\mathbf{k}l'\sigma B} + \hat{c}_{\mathbf{k}l\sigma B}^\dagger \hat{c}_{\mathbf{k}l'\sigma A}) \\ &\quad - \mu \sum_{\mathbf{k}l\sigma} (q_\sigma^s \hat{n}_{\mathbf{k}l\sigma A} + q_\sigma^s \hat{n}_{\mathbf{k}l\sigma B}) + \frac{L}{2} \sum_{I_1,I_4} \bar{E}_{I_1,I_4}^A \langle \hat{m}_{I_1,I_4}^A \rangle_0 + \frac{L}{2} \sum_{I_1,I_4} \bar{E}_{I_1,I_4}^B \langle \hat{m}_{I_1,I_4}^B \rangle_0, \end{aligned} \quad (56)$$

where

$$Q = q_{\uparrow}q_{\downarrow} - \bar{q}_{\uparrow}\bar{q}_{\downarrow}. \quad (57)$$

It should be noted that the sums in (56) are taken over all $L/2$ independent \mathbf{k} states. As before, we apply the SGA method which leads to the effective Hamiltonian with the statistical-consistency constraints of the form

$$\begin{aligned} \hat{K}_{\lambda} = & \hat{K}_{\text{GA}} - \lambda_S \left[\sum_{\mathbf{k}l\sigma} \frac{1}{2} \sigma (\hat{n}_{\mathbf{k}l\sigma A} - \hat{n}_{\mathbf{k}l\sigma B}) - 2L S_{0|S}^z \right] \\ & - \lambda_+ \left[\sum_{\mathbf{k}} (\hat{A}_{\mathbf{k}1A} + \hat{A}_{\mathbf{k}-1B}) - L \Delta_+^0 + \text{h.c.} \right] \\ & - \lambda_- \left[\sum_{\mathbf{k}} (\hat{A}_{\mathbf{k}-1A} + \hat{A}_{\mathbf{k}1B}) - L \Delta_-^0 + \text{h.c.} \right] \\ & - \lambda_n \left[\sum_{\mathbf{k}l\sigma} (q_{\sigma}^s \hat{n}_{\mathbf{k}l\sigma A} + q_{\sigma}^s \hat{n}_{\mathbf{k}l\sigma B}) - L n_G \right]. \end{aligned} \quad (58)$$

Introducing now the eight-component composite operator

$$\hat{\mathbf{f}}_{\mathbf{k}\sigma}^{\dagger} \equiv (\hat{c}_{\mathbf{k}1\sigma A}^{\dagger}, \hat{c}_{\mathbf{k}2\sigma A}^{\dagger}, \hat{c}_{\mathbf{k}1\sigma B}^{\dagger}, \hat{c}_{\mathbf{k}2\sigma B}^{\dagger}, \hat{c}_{-\mathbf{k}1\sigma A}, \hat{c}_{-\mathbf{k}2\sigma A}, \hat{c}_{-\mathbf{k}1\sigma B}, \hat{c}_{-\mathbf{k}2\sigma B}), \quad (59)$$

we can write down the effective Hamiltonian \hat{K}_{λ} in the following form:

$$\begin{aligned} \hat{K}_{\lambda} = & \frac{1}{2} \sum_{\mathbf{k}\sigma} \hat{\mathbf{f}}_{\mathbf{k}\sigma}^{\dagger} \hat{\mathbf{M}}_{\mathbf{k}\sigma} \hat{\mathbf{f}}_{\mathbf{k}\sigma} - (\mu + \lambda_n)(q_{\uparrow}^s + q_{\downarrow}^s)L \\ & + 2L\lambda_+ \Delta_+^0 + 2L\lambda_- \Delta_-^0 + 2L\lambda_S S_{0|S}^z + L\lambda_n n_G \\ & + \frac{L}{2} \sum_{I_1, I_4} \bar{E}_{I_1, I_4}^A \langle \hat{m}_{I_1, I_4}^A \rangle_0 + \frac{L}{2} \sum_{I_1, I_4} \bar{E}_{I_1, I_4}^B \langle \hat{m}_{I_1, I_4}^B \rangle_0, \end{aligned} \quad (60)$$

where the explicit form of the 8×8 matrix is

$$\hat{\mathbf{M}}_{\mathbf{k}\sigma} = \begin{pmatrix} \eta_{\sigma}^{-} & 0 & Q\epsilon_{\mathbf{k}} & Q\epsilon_{\mathbf{k}12} & 0 & \lambda_{\sigma}^A & 0 & 0 \\ 0 & \eta_{\sigma}^{-} & Q\epsilon_{\mathbf{k}12} & Q\epsilon_{\mathbf{k}} & -\lambda_{\sigma}^A & 0 & 0 & 0 \\ Q\epsilon_{\mathbf{k}} & Q\epsilon_{\mathbf{k}12} & -\eta_{\sigma}^{+} & 0 & 0 & 0 & 0 & \lambda_{\sigma}^B \\ Q\epsilon_{\mathbf{k}12} & Q\epsilon_{\mathbf{k}} & 0 & -\eta_{\sigma}^{+} & 0 & 0 & -\lambda_{\sigma}^B & 0 \\ 0 & -\lambda_{\sigma}^A & 0 & 0 & -\eta_{\sigma}^{-} & 0 & -Q\epsilon_{\mathbf{k}} & -Q\epsilon_{\mathbf{k}12} \\ \lambda_{\sigma}^A & 0 & 0 & 0 & 0 & -\eta_{\sigma}^{-} & -Q\epsilon_{\mathbf{k}12} & -Q\epsilon_{\mathbf{k}} \\ 0 & 0 & 0 & -\lambda_{\sigma}^B & -Q\epsilon_{\mathbf{k}} & -Q\epsilon_{\mathbf{k}12} & \eta_{\sigma}^{+} & 0 \\ 0 & 0 & \lambda_{\sigma}^B & 0 & -Q\epsilon_{\mathbf{k}12} & -Q\epsilon_{\mathbf{k}} & 0 & \eta_{\sigma}^{+} \end{pmatrix} \quad (61)$$

and

$$\begin{aligned} \lambda_{\uparrow}^A = \lambda_{\downarrow}^B & \equiv \lambda_+, \quad \lambda_{\downarrow}^A = \lambda_{\uparrow}^B \equiv \lambda_-, \\ \eta_{\sigma}^{-} & = -\frac{1}{2}\sigma\lambda_S - q_{\sigma}^s(\mu + \lambda_n), \quad \eta_{\sigma}^{+} = -\frac{1}{2}\sigma\lambda_S + q_{\sigma}^s(\mu + \lambda_n). \end{aligned} \quad (62)$$

Table 3. Number of equations that have to be solved in the case of all phases considered here. To reduce the number of equations for particular phases we have used certain symmetry relations regarding the mean-field parameters, the Lagrange multipliers and the variational parameters.

Phase	A	A1 + FM	SC + AF	AF	NS	FM
No. of equations	16	17	22	12	8	13

Table 4. Acronyms representing the considered phases.

A	Pure type A superconducting phase
A1 + FM	Superconducting phase type A1 coexisting with ferromagnetism
SC + AF	Superconducting phase coexisting with antiferromagnetism
FM	Pure ferromagnetic phase
AF	Pure antiferromagnetic phase
NS	Paramagnetic phase

Diagonalization of (61) leads to the quasi-particle energies $E_{\mathbf{k}l\sigma}$ ($l = 1, 2, 3, \dots, 8$). The corresponding grand potential function F_λ per atomic site now has the form

$$\begin{aligned}
 F_\lambda = & -\frac{2}{L\beta} \sum_{\mathbf{k}l\sigma} \ln [1 + e^{-\beta E_{\mathbf{k}l\sigma}}] - \mu(q_\uparrow^s + q_\downarrow^s) \\
 & + 2\lambda_+ \Delta_+^0 + 2\lambda_- \Delta_-^0 + 2\lambda_S S_{0|s}^z + (\lambda_n + \mu)n_G \\
 & + \frac{L}{2} \sum_{I_1, I_4} \bar{E}_{I_1, I_4}^A \langle \hat{m}_{I_1, I_4}^A \rangle_0 + \frac{L}{2} \sum_{I_1, I_4} \bar{E}_{I_1, I_4}^B \langle \hat{m}_{I_1, I_4}^B \rangle_0.
 \end{aligned} \tag{63}$$

As before, we minimize the F_λ function to determine the values of the mean fields, the variational parameters and the Lagrange parameters. The necessary conditions for the minimum are again expressed by (45) and (46). In the subsequent discussion, we consider also the pure antiferromagnetic phase (AF), for which $S_{G|s}^z \neq 0$ but $\Delta_+ = \Delta_- \equiv 0$. The number of equations that need to be solved is different for different phases considered in this work. In table 3 we show how many equations are included in (45) and (46) for all phases discussed.

3. Results and discussion

Equations (45) and (46) have been solved numerically for all phases by means of the hybrid1 subroutine from the MINPACK library, which performs a modification of the Powell hybrid method. The maximal estimated error of the procedure was set to 10^{-7} . The derivatives in equation (45) and (46) were computed by using a five-step stencil method with the step equal to $x = 10^{-4}$. For the sake of clarity, we have provided the acronyms representing the phases considered here in table 4.

We concentrate now on the detailed numerical analysis of the phase diagram and the microscopic characterization of the stable phases. Keeping in mind that for 3d orbitals $U' = U - 2J$, one obtains the HF condition for the pairing to occur, $U < 3J$ (see [22]). We discuss thus first and foremost the limit $U < 3J$, as it allows for a direct comparison of SGA with the

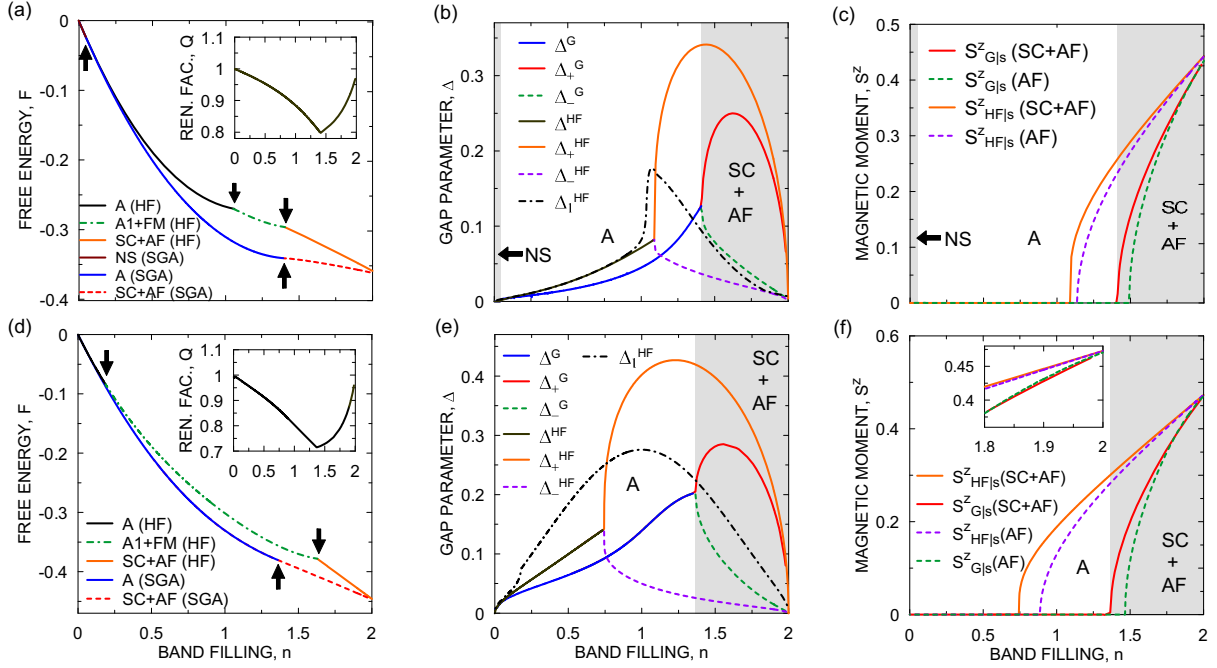


Figure 1. Stable phases evolution versus band filling. The superconducting gap parameter, magnetic moment and free energies as a function of band filling both for the HF and SGA, for $J = 0.299$: (a)–(c) and $J = 0.4545$: (d)–(f). The results are for $\beta_h = 0.0$. The shaded regions represent the stability regions of the respective phases according to the SGA calculations. In figures (a) and (d), we show only the free energies of stable phases. The arrows in (a) and (d) mark the transitions points between phases.

HF solution. In this manner we can single out explicitly the role of correlations in stabilizing the relevant phases. One should note that in the considered regime ($U < 3J$) we have a model with intraatomic interorbital attractions leading to spin-triplet pairs. As the main attractive force is of intraatomic nature, we focus here on the local (s-wave) type of pairing only. In other words, as we discuss the situation with no or small hybridization, the intersite part of the pairing can be disregarded.

The calculations have been carried out for $U' = U - 2J$, $U = 2.2J$, $k_B T/W = 10^{-4}$. This leaves us still with three independent microscopic parameters in our model: n_G , J and β_h . All the energies have been normalized to the bare bandwidth $W = 8|t|$ (as we consider the square lattice with nearest-neighbor hopping). For comparison, we also show the results calculated by means of the combined HF–BCS \equiv HF approximation. This method is described in detail in our previous paper for the same model as considered here. We can also reproduce the HF results by using the Gutzwiller method described in this work and setting $\lambda_{I,I'} = \delta_{I,I'}$.

In figure 1, we display the free energy, superconducting gaps and magnetic moments for the two values $J = 0.299$ and 0.4545 . As one can see from the free-energy plots (figures 1(a) and (d)), below some certain value of band filling, the pure superconducting phase of type A is stable for the SGA method. The increase of the number of electrons in the system enhances the gap in this region (figures 1(b) and (e)). Above the critical band filling n_c , the staggered moment structure is created and a division into two gap parameters (Δ_+ and Δ_-) appears, as can be seen in figures 1(b), (c), (e) and (f). In this regime the SC + AF phase becomes stable.

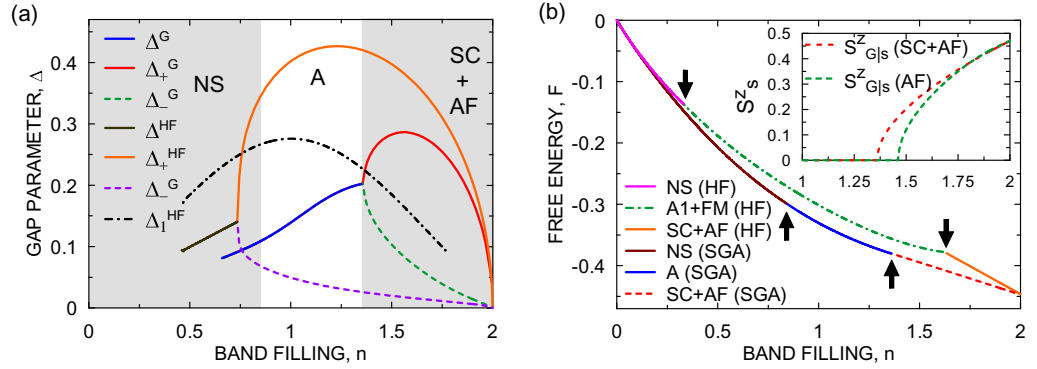


Figure 2. The superconducting gaps (a) and the free energies (b) as a function of band filling for $J = 0.4545$ and $\beta_h = 0.1$. The shaded regions represent the stability of respective phases according to the SGA calculations. The vertical arrows mark the phase borders.

When approaching half filling, both gaps gradually approach zero and for $n = 2$ we are left with a pure AF phase, which is of Slater insulating type evolving toward the Mott–Hubbard insulating state with the increasing U . As the staggered magnetic moment is rising (with the increase of n_G), the renormalization factor is approaching unity (cf insets to figures 1(a) and (d)). This is a consequence of the fact that for large values of S_G^z , the configurations with two electrons of opposite spin, on the same orbital, are ruled out.

Comparing figures 1(a)–(c) with figures 1(d)–(f) one sees that by increasing J we make the value of n_c smaller. However, the decrease in n_c is not as significant in SGA as it is in the HF case. In general, the results presented in figures 1(b), (e), (c) and (f) look similar from the qualitative point of view for both methods. For SGA, the onset of antiferromagnetically ordered phase appears closer to half filling than for the HF method. Another difference between HF and SGA is that for the former the staggered moment in the SC + AF phase is increased by the appearance of SC for the whole range of band fillings, whereas in SGA calculations the staggered moment is slightly stronger in the AF phase than in the SC + AF phase for a small region close to the half-filled situation (inset of figure 1(f)).

Significant differences between HF and SGA can be seen in figures 1(c) and (f). While changing the band filling from 0 to 2, in the case of SGA calculations, we move consecutively through the regions of stability of NS (for $J = 0.299$), A, SC + AF phases, and for $n = 2$ we have pure antiferromagnetism. The situation is different in the HF approximation, where in between the regions of stability of A and SC + AF phase, we have also the stable A1 + FM phase. It should be also noted that the free energy calculated in SGA is lower than the one for the HF situation, as one should expect, since the correlations are accounted more accurately in the former method. It is also very interesting that having the system with $U < 3J$, no pure ferromagnetism appears in this canonical model of itinerant magnetism.

In figure 2, we present the results for the case with non-zero hybridization parameter, $\beta_h = 0.1$. In this case there are no pure superconducting solutions below some certain value of the band filling (cf figure 2(a)) and an extended region of NS stability occurs. The influence of the hybridization on the antiferromagnetically ordered phases is weak, as can be seen more clearly in figure 3. The changes in the superconducting gap and the magnetic moment in the coexistent phase triggered by the hybridization are quite small even for larger values of β_h .

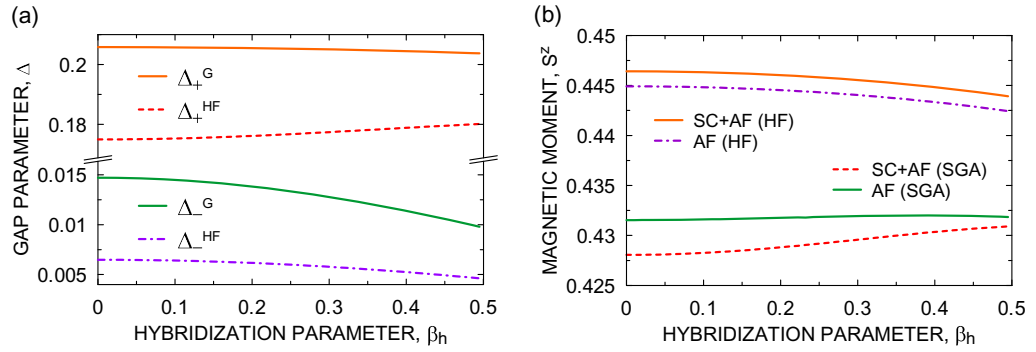


Figure 3. The superconducting gaps and magnetic moment as a function of the hybridization strength, β_h , for $n = 1.9$, $J = 0.4545$, for the case of SC + AF and AF phases.

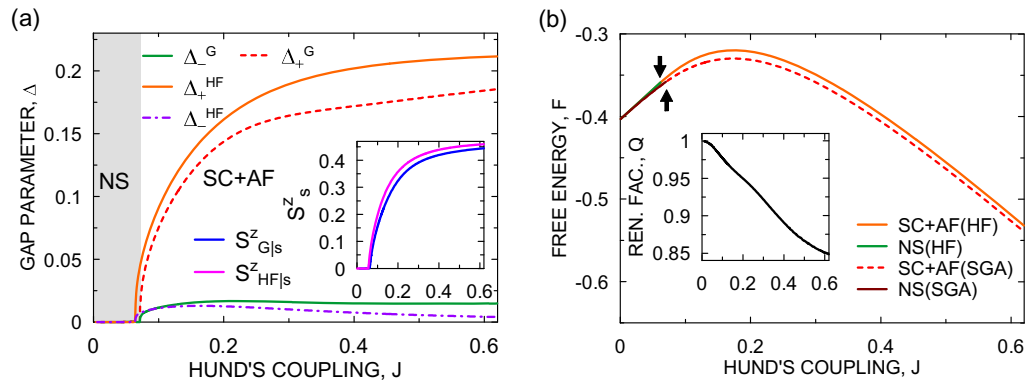


Figure 4. The superconducting gaps in the SC + AF phase (a) and free energies of stable phases (b) as a function of Hund's coupling for $n = 1.9$ and $\beta_h = 0.1$. The shaded region represent the stability of NS phase according to the SGA results.

It should be noted that the hybridization leads to inequivalent bands. Hence the pairing is robust against the Fermi wave vector mismatch for the carriers composing the Cooper pair, at least not for too large β_h .

Next, we discuss the J dependence of the superconducting gap, the free energy and the magnetic moment for selected values of band filling. As in the case of n -dependences the gap parameters and the magnetic moments in both SGA and HF approximation are qualitatively similar. In figure 4, we can see that for $n = 1.9$ even the free-energy plots and regions of stability of certain phases are comparable for both calculation schemes used. For the quarter-filled case (cf figure 5) the A1 + FM phase is stable above some value of J , according to the HF results. However, this is not the case in the SGA approximation, where the A phase has lower free energy even than the saturated ferromagnetic phase coexisting with superconductivity. Comparing figures 5(b) and (d) (as well as 1(d) and 2(b)) one sees that the region of stability of the A phase narrows down in favor of the NS phase, due to the influence of hybridization. For the sake of completeness we provide in table 5 the exemplar values of the principal physical quantities for the two values of the band filling, $n = 1.0$ and $n = 1.9$. The pure A Phase, as well as the coexistent AF + SC phase are stable then.

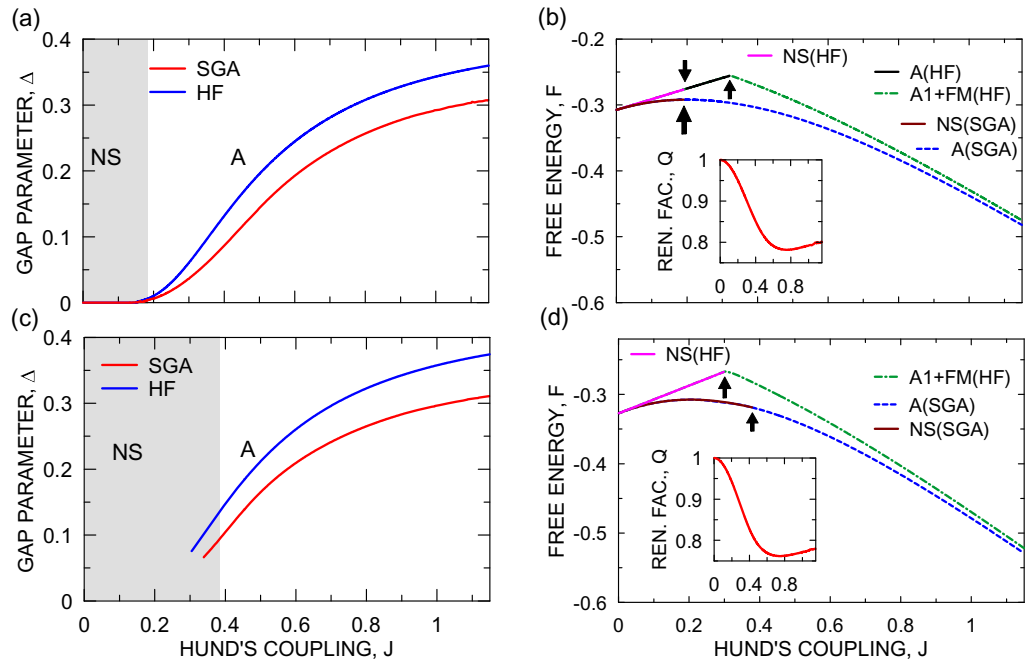


Figure 5. The superconducting gaps in the A phase as a function of the Hund's coupling for $n = 1.0$ ((a)-for $\beta_h = 0.0$ and (c)-for $\beta_h = 0.1$) and free energies of stable phases corresponding to SGA and HF approximations ((b)-for $\beta_h = 0.0$ and (d)-for $\beta_h = 0.1$). The shaded regions represent the stability of the NS phase according to the SGA. The vertical arrows mark the border points between respective phases. Insets: bandwidth renormalization factor for $\beta_h = 0$ (upper) and $\beta_h = 0.1$ (lower).

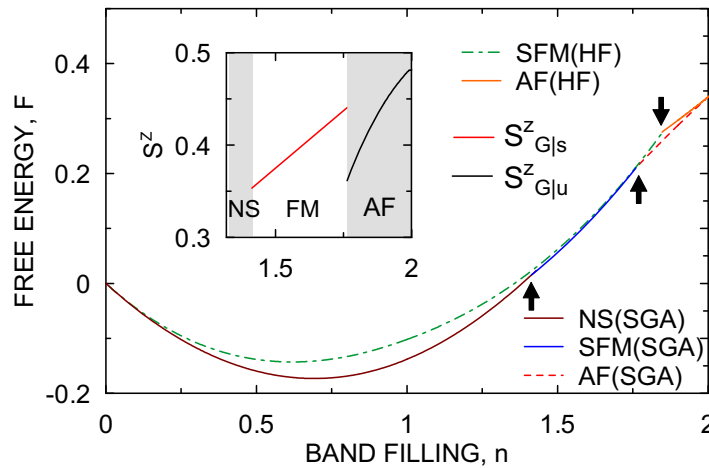


Figure 6. The free energies of the stable phases for SGA and HF methods for $J = 0.4$, $U = 1.6$ and $\beta_h = 0$. The shaded regions in the inset mark the stability of certain phases according to the SGA approach. Note the appearance of ferromagnetic phase for $U = 4J$ (i.e. for $U > 3J$) in the filling range 1.45–1.75, sandwiched in between paramagnetic and antiferromagnetic phases.

Table 5. Exemplary values of the order parameters, the chemical potential, the free energy and the band renormalization factors corresponding to the considered phases, for two different sets of values of the microscopic parameters n and J . The underlined values correspond to the stable phases. The numerical accuracy is on the level of the last digit specified.

Parameter	Phase	$n = 1.0$	$n = 1.9$
		$J = 0.299$	$J = 0.299$
Δ	A	<u>0.045 002 7</u>	0.170 194 0
Δ	A1 + FM	0.042 674 9	0.130 766 4
Δ_+	SC + AF	–	<u>0.163 899 2</u>
Δ_-	SC + AF	–	<u>0.016 186 8</u>
S_u^z	A1 + FM	0.000 317	0.109 267 4
S_s^z	SC + AF	–	<u>0.390 273 8</u>
S_s^z	AF	–	0.388 589 9
μ	A	<u>–0.138 237 7</u>	0.160 786 01
μ	NS	–0.137 764 9	0.187 596 4
μ	A1 + FM	–0.137 970 0	0.182 225 14
μ	SC + AF	–	<u>–0.042 114 4</u>
μ	AF	–	–0.089 396 3
F	A	<u>–0.310 609 1</u>	–0.311 838 1
F	NS	–0.310 514 5	–0.299 251 6
F	A1 + FM	–0.310 558 6	–0.302 025 4
F	SC + AF	–	<u>–0.357 654 2</u>
F	AF	–	–0.350 973 1
Q_\uparrow	A1 + FM	0.884 577 6	0.675 161 9
Q_\downarrow	A1 + FM	0.883 925 1	0.628 245 2
Q	A	<u>0.884 513 6</u>	0.673 637 3
Q	NS	0.884 034 0	0.642 108 9
Q	SC + AF	–	<u>0.921 122 4</u>
Q	AF	–	0.929 356 7

It is important to check whether the itinerant magnetic phases are stable in the regime $U' > J$ ($U > 3J$), i.e. when the superconductivity is absent in the HF approximation. For this purpose, in figure 6 we provide the band-filling dependence of the free energy corresponding to stable phases for $U = 4J$. Indeed, the paramagnetic and the magnetically ordered phases are stable for both methods of calculations. Therefore, for $U > 3J$ we recover the magnetic phase diagram for this model, which was considered originally only in the context of magnetism. The free energy of the saturated ferromagnetic phase calculated by the SGA approach is very close to the one obtained by the HF approach. This is again caused by the circumstance that in the saturated state all the spins are parallel and the double occupancies on the same orbital are absent. In this situation, the intra-orbital Coulomb interaction is automatically switched off. For the sake of completeness, we have plotted in figures 7(a) and (b) the double occupancy probability d , both in HF (d^0) and SGA (d^G) treatments. One should note a drastic reduction of d in SGA with the increasing J (and hence U). This is the reason why we have neglected both the so-called correlated-hopping and the pair-hopping terms in the starting Hamiltonian.

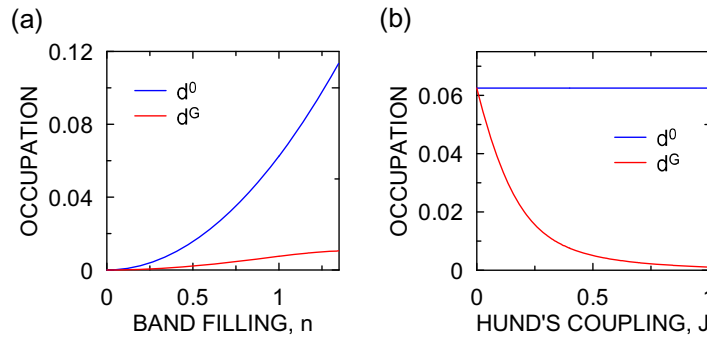


Figure 7. The average double occupancies $d^0 = \langle \hat{n}_{il\uparrow} \hat{n}_{il\downarrow} \rangle_0$ and $d^G = \langle \hat{n}_{il\uparrow} \hat{n}_{il\downarrow} \rangle_G$ versus band filling (a) and Hund's coupling (b) corresponding to the normal state (NS) for the parameters: $J = 0.4$, $U = 1.6$, $\beta_h = 0$ —(a) and $U = 4J$, $n = 1$, $\beta_h = 0$ —(b).

It would be interesting to determine the stability of the coexistent phases in this regime ($U' > J$). Work along this line is in progress.

4. Conclusions

The principal purpose of this paper was to formulate a many-particle method which allows us to investigate the spin-triplet real-space pairing in correlated system with an orbital degeneracy. To this end, we have carried out a detailed analysis using the SGA for the two-band degenerate Hubbard model with the spin-triplet superconductivity and itinerant magnetism included, both treated on equal footing. Also, in our approach we have discussed explicitly the nature of ordered phases. The previous analysis [31, 47] carried out in the dynamic mean-field approach addressed only the instability of the normal phase against the formation of the pure paired states. We compare our results with those coming from the HF approximation amended with the BCS approach. The obtained Hund's coupling and band-filling dependences of the magnetic moment and the superconducting gap parameters are often similar from the qualitative point of view with those evaluated by means of the HF approximation. However, the stability regions of the considered phases are significantly different for the two applied methods. In SGA, the stable coexisting superconducting-ferromagnetic phase is absent while it appears in the HF approximation in a certain range of J and n values. Furthermore, the coexistence of the paired state with antiferromagnetism appears much closer to the half-filled situation in SGA than in HF approximation. For $n = 2$, the superconductivity disappears and only the pure antiferromagnetism survives; this state can be termed as a correlated Slater–Mott-insulator state, as it evolves gradually into the Mott–Hubbard insulating state with increasing $U > 1$ and $S_{G|s}^z \rightarrow 1/2$.

The influence of hybridization for both approximations is similar. With an increase of the β_h parameter, the region of stability of the superconducting type-A phase narrows down in favor of the NS state. On the other hand, the antiferromagnetic phase is not affected in any significant manner by an increase of β_h .

The band renormalization factors approach unity as the interaction constants J , U and U' tend to zero, which represents an additional test of correctness of our numerical results.

Generally, in the weak-coupling limit our present results reduce to those obtained in HF approximation analyzed by Zegrodnik and Spalek in [22], as it should be.

It is important to emphasize that for both approaches (SGA and HF) the phase diagrams have been obtained for $U < 3J$, i.e. for a relatively low value of the Hubbard interaction U , or equivalently, for a relatively high value of the Hund's rule exchange integral. We call this regime the one with attractive pairing interaction. A complete analysis of the present model would require studying the stability of the spin-triplet superconductivity and its coexistence with magnetic ordering in the complementary regime $U > 3J$, where the magnetism may be favored against superconductivity. This regime has been the subject in a number of earlier papers [24, 48, 49], as then both the intraorbital, as well as the interorbital, interaction is repulsive and leads to magnetic ordering in a natural manner. We should see progress along this line soon.

Acknowledgments

Discussions with Jakub Jędrak and Jan Kaczmarczyk are gratefully acknowledged. MZ has been partly supported by the EU Human Capital Operation Program, Polish project no. POKL.04.0101-00-434/08-00. JS acknowledges the financial support from the Foundation for Polish Science (FNP) within the project TEAM. The grant MAESTRO from the National Science Center (NCN), No. DEC-2012/04/A/ST3/00342 was helpful for the PL-DE cooperation within the present project on a unified approach to magnetism and superconductivity in correlated fermion systems.

References

- [1] Maeno Y, Hashimoto H, Yoshida K, Nishizaki S, Fujita T, Bednorz J G and Lichtenberg F 1994 *Nature* **372** 532
- [2] Maeno Y 2000 *Physica B* **281–282** 865
- [3] Saxena S S *et al* 2000 *Nature* **406** 587
- [4] Huxley A, Sheikin I, Ressouche E, Kemovanois N, Braithwaite D, Calemczuk R and Flouquet J 2001 *Phys. Rev. B* **63** 144519
- [5] Tateiwa N, Kobayashi T C, Hanazono K, Amaya K, Haga Y, Settai R and Onuki Y 2001 *J. Phys.: Condens. Matter* **13** 117
- [6] Kobayashi T C, Fukushima S, Hidoka H, Kotegawa H, Akazawa T, Yamamoto E, Haga Y, Settai R and Onuki Y 2006 *Physica B* **378–380** 355
- [7] Huy N T, Gasparini A, de Nijs D E, Huang Y, Klaasse J C P, Gortenmulder T, de Visser A, Hamann A, Görlach T and Löhneysen H v 2007 *Phys. Rev. Lett.* **99** 067006
- [8] Slooten E, Naka T, Gasparini A, Huang Y K and de Visser A 2009 *Phys. Rev. Lett.* **103** 097003
- [9] For a review, see de Visser A 2010 *Encyclopedia of Materials Science: Science and Technology* (Amsterdam: Elsevier) pp 1–6
- [10] Geibel C *et al* 1991 *Z. Phys. B* **83** 305
- [11] Schröder A, Lussier J G, Gaulin B D, Garrett J D, Buyers W J L, Rebelski L and Shapiro S M 1994 *Phys. Rev. Lett.* **72** 136
- [12] Ishida K *et al* 2002 *Phys. Rev. Lett.* **89** 037002
- [13] Aeppli G, Bishop D, Broholm C, Bucher E, Siemensmeyer K, Steiner M and Stüsser N 1989 *Phys. Rev. Lett.* **63** 676
- [14] Tou H, Kitaoka Y, Asayama K, Kimura N, Onuki Y, Yamamoto E and Maezawa K 1996 *Phys. Rev. Lett.* **77** 1374

- [15] Klejnberg K and Spałek J 1999 *J. Phys.: Condens. Matter* **11** 6553
- [16] Klejnberg K and Spałek J 2000 *Phys. Rev. B* **61** 15542
- [17] Spałek J 2001 *Phys. Rev. B* **63** 104513
- [18] Spałek J, Wróbel P and Wójcik W 2003 *Physica C* **387** 1
- [19] Shen S-Q 1998 *Phys. Rev.* **57** 6474
- [20] Zegrodnik M and Spałek J 2012 *Acta Phys. Pol. A* **121** 1051
- [21] Zegrodnik M and Spałek J 2012 *Acta Phys. Pol. A* **121** 801
- [22] Zegrodnik M and Spałek J 2012 *Phys. Rev. B* **86** 014505
- [23] Bünemann J and Weber W 1997 *Phys. Rev. B* **55** 4011
- [24] Bünemann J, Weber W and Gebhard F 1998 *Phys. Rev. B* **57** 6896
- [25] Bünemann J, Gebhard F, Ohm T, Weiser S and Weber W 2005 *Frontiers in Magnetic Materials* ed A Narlikar (Berlin: Springer) pp 117–51
- [26] Jędrak J and Spałek J 2010 *Phys. Rev. B* **81** 073108
- [27] Kaczmarczyk J and Spałek J 2011 *Phys. Rev. B* **84** 125140
- [28] Howczak O and Spałek J 2012 *J. Phys.: Condens. Matter* **24** 205602
- [29] Jędrak J, Kaczmarczyk J and Spałek J 2011 arXiv:1008.0021v2 [cond-mat.str-el]
- [30] Sano K and Ōno Y 2003 *J. Phys. Soc. Japan* **72** 1847
- [31] Han J E 2004 *Phys. Rev. B* **70** 054513
- [32] Hotta J and Ueda K 2004 *Phys. Rev. Lett.* **92** 107007
- [33] Dai X, Fang Z, Zhou Y and Zhang F-C 2008 *Phys. Rev. Lett.* **101** 057008
- [34] Lee P A and Wen X-G 2008 *Phys. Rev. B* **78** 144517
- [35] Imai Y, Wakabayashi K and Sigrist M 2012 *Phys. Rev. B* **85** 174532
- [36] Gorshkov A V, Hermele M, Gurarie V, Xu C, Julienne P S, Ye J, Zoller P, Demler E, Lukin M D and Rey A M 2010 *Nature Phys.* **6** 289
- [37] Cherng R W, Rafael G and Demler E 2007 *Phys. Rev. Lett.* **99** 130406
- [38] Wu C, Hu J and Zhang S-C 2009 *Int. Mod. Phys. B* **24** 311
- [39] Zwicknagl G 2006 *J. Phys. Soc. Japan* **75S** 226 and references therein
- [40] For a recent review, see Knebel G, Buhot J, Aoki D, Laperot G, Raymond S, Ressouche E and Flouquet J 2011 *Phys. J. Soc. Japan* **80** SA001
- [41] Howczak O, Kaczmarczyk J and Spałek J 2012 arXiv:1209.0621
- [42] Howczak O, Kaczmarczyk J and Spałek J 2013 *Phys. Status Solidi b* **250** 609
- [43] Fay D and Appel J 1980 *Phys. Rev. B* **22** 3173
- [44] Layzer A and Fay D 1971 *Inter. J. Magn.* **1** 135
- [45] Anderson P W and Brinkman W F 1977 *The Physics of Liquid and Solid Helium* ed K H Bennemann and J B Ketterson (New York: Wiley) p 177ff
- [46] Griffith J S 1971 *The Theory of Transition Metals and Ions* (Cambridge: Cambridge University Press) cf appendix 6
- [47] Bünemann J, Gebhard F, Schickling T and Weber W 2010 *Phys. Status Solidi b* **248** 203
- [48] Bünemann J, Gebhard F and Thul R 2003 *Phys. Rev. B* **67** 075103
- [49] Sakai S, Arita R and Aoki H 2004 *Phys. Rev. B* **70** 172504
- [50] Kuneš J, Leonov I, Kollar M, Byczuk K, Anisimov V I and Vollhardt D 2010 *Eur. Phys. J. Spec. Top.* **180** 5
- [51] Deng X Y, Wang L, Dai X and Fang Z 2009 *Phys. Rev. B* **79** 075114